INSTITUTE OF PHYSICS PUBLISHING MEASUREMENT SCIENCE AND TECHNOLOGY
Meas. Sci. Technol. **17** (2006) 477–482 doi:10.1088/0957-0233/17/3/S03

3D roughness evaluation of cylinder liner surfaces based on structure-oriented parameters

A Weidner, J Seewig and E Reithmeier

Institute for Measurement and Control, University of Hannover, Nienburger Str. 17, 30167 Hannover, Germany

E-mail: weidner@imr.uni-hannover.de

Received 1 July 2005, in final form 20 November 2005
Published 31 January 2006
Online at stacks.iop.org/MST/17/477

Abstract
Modern cylinder liner manufacturing processes such as MMC casting, laser honing and laser exposure allow a design of cylinder liner surfaces to meet common development goals like less air pollution and reduced fuel and oil consumption. These goals are reached by aimed insertion of function-relevant structures on the micrometre scale into the surface. Because of these function-relevant structures, the commonly used 2D roughness parameters like Ra and Rz cannot describe the functional behaviour of these surfaces. To describe these surfaces it is necessary to extend the roughness evaluation into the third dimension: $z = z(x, y)$. This paper proposes a 3D roughness evaluation method based on morphological algorithms like the watershed transform to detect and separate the function-relevant structures. Every detected structure is described by a set of structural parameters. Statistical combining of these structural parameters provides a functional characterization of the complete measured surface. The possibilities provided by this flexible method of surface evaluation are shown with a calculation of honing angles.

Keywords: surface roughness, microstructure detection algorithm, 3D roughness parameters, honing angle detection

1. Introduction

Many technical surfaces provide their function through specifically designed structures in the roughness scale. A great application field for this kind of surface is tribology. For cylinder liners, a range of manufacturing methods exist which allow through aimed insertion of these function crucial structures a design of the tribological behaviour between piston ring and cylinder liner.

These function crucial structures could be honing grooves as to be seen in conventional honing. Modern manufacturing methods extend this structures to hard material crystals (metal matrix composites (MMC) [1]), laser holes (laser honing [2]) and opened graphite accumulations (laser exposure [3]).

Commonly used 2D roughness parameters could not describe the additional function of these structured surfaces. Even modern 3D surface evaluations [4, 5] provide only a limited functional description of these surfaces. The roughness evaluation proposed in this paper tries to identify the function crucial structures and describe them with structural parameters. Statistical combination of these parameters provides intuitive information on the measured surface as it is shown with a calculation of honing angles.

2. Basic principle

Natural surfaces have a fractal character [6]. By lowering the measurement scale new details and therefore new structures evolve. With noisy measurement systems for this kind of surface, it is very difficult to tell the difference between real surface structures and measurement noise.

Cylinder liner surfaces show a fractal character in the roughness domain too. Reproducible evaluation of these

0957-0233/06/030477+06$30.00

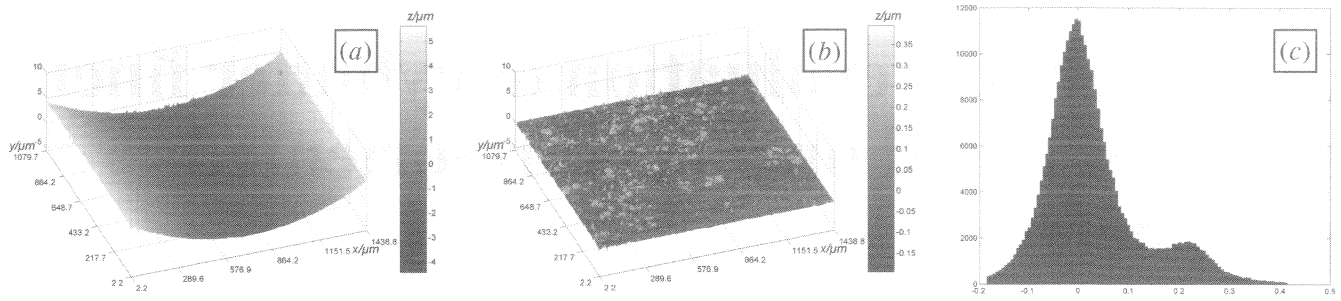

Figure 1. Alignment of the surface: (*a*) original surface; (*b*) aligned surface; (*c*) histogram of the aligned surface with reference zero set to the highest density of material.

multiscalar surfaces depends on hierarchical models, which can be summarized by the change tree proposed by Scott [7]. Due to measurement noise of especially optical profilers, noise caused by the measurement instrument overlays the roughness of the surface, which makes it difficult to differentiate between relevant and irrelevant structures. Good differentiation results with MST devices [8] are achieved with a height pruning [9] of irrelevant structures. Barre and Lopez [10] propose for 3D roughness evaluations a differentiation based on the areal size of the structures.

The method proposed in this paper uses the linear material ratio curve (also referred to as the Abbott curve [11]). Roughness evaluation based on the linear material ratio curve [12] divides the surface into three layers: valleys, peaks and the core region. In this paper, this evaluation is extended by separating the integral parameters for the valley and peak regions into a number of structural parameters for the single spatially distributed valley and peak structures.

The structures are separated against the core region by their steepest connected edge which is realized with a marker-based watershed transform on the gradient of the surface. The identification of the structures and, therefore, the generation of the markers is done with local thresholds. The instability of the watershed transform of a gradient due to measurement noise is lowered by increasing the size of the structure markers and with that decreasing the range where the watershed lines can settle.

The detected structures are further described with structural parameters [13]. The reduction of the oversegmented result is done by using a combination of meaningful structural parameters. For MMC surfaces, the areal size of the structures turned out to be very selective to distinguish between relevant and irrelevant structures. With structural parameters the distinction could be very intuitively done by the designing engineer who is familiar with the characteristics of the surface.

3. Detection

The first step of the detection is the alignment of the surface (F-operator). Form and waviness of the surface should be removed within this step, leaving only the roughness for further processing. With this alignment the reference of the vertical direction is set to that point of the height scale where most of the material is located (figure 1(*c*)). Robust Gaussian regression filters and alignment operators [14] realize this in a very suitable way. The cut-off wavelength λ_c should be chosen with respect to interesting structures [15].

By setting the reference to the highest material density the point of reference zero approximates the core region of the surface very well. Every point above this reference zero is a potential peak structure, every point below is a potential valley structure.

The detection of a peak is done with the proposed algorithm used on the original surface. Valley structures are detected with the same algorithm used on the inverted surface. Subsequently, the algorithm is described for the case of a peak structure detection.

Combining all adjacent potential peak structure points into a single region provides a number of autonomous regions of the surface. The adjacency of data points is defined over a four-connected neighbourhood graph [16].

The actual structure detection is realized with a marker-based watershed transform. The structure marker is calculated separately for every autonomous region. With respect to batwings, pepper and peak noise of optical topography measuring systems a robust method to derive the marker is chosen. All points of a region are sorted by their height. Five per cent of the highest points are dropped and the height $h_{5\%}$ of the highest remaining point is used. Every region point higher than $0.75h_{5\%}$ is used as a marker for a potential structure.

Combining adjacent marker points via the four times neighbourhood leads to connected structure markers of the autonomous region. It is possible that there could be more than one structure marker per autonomous region.

In the described case of a peak structure detection, all points of the surface with a height below or equal to zero generate the background marker. With this definition, the background marker contains all points that are for sure not peak structure points.

The subsequent marker-based watershed transform uses the structure and the background markers as initial sources to find the watershed lines. The FIFO-based watershed algorithm [16] is extended to use markers and avoid the occurrence of watershed regions. Furthermore, some watershed algorithm-dependent preprocessing of the markers is necessary like avoiding connected background and structure markers and generating a measurement field border marker.

The watershed transform is used on the Beucher gradient [16] of the surface. The Beucher gradient ρ_B is the difference between the dilation δ_B and the erosion ε_B with a structuring element B (diamond) of the surface

$$\rho_B = \delta_B - \varepsilon_B. \tag{1}$$

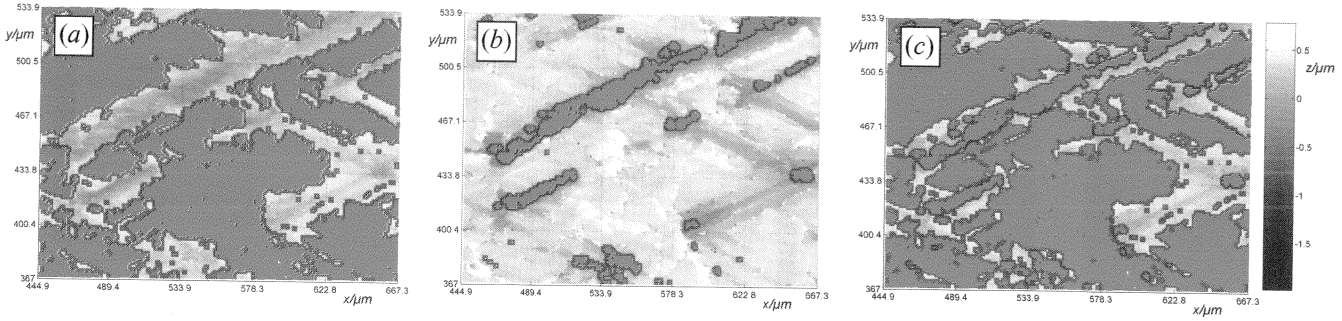

Figure 2. Detection of valley structures: (*a*) background marker with autonomous regions; (*b*) structure (valley) marker; (*c*) background and structure markers combined into one marker image. The watershed lines can only settle in the space between the markers.

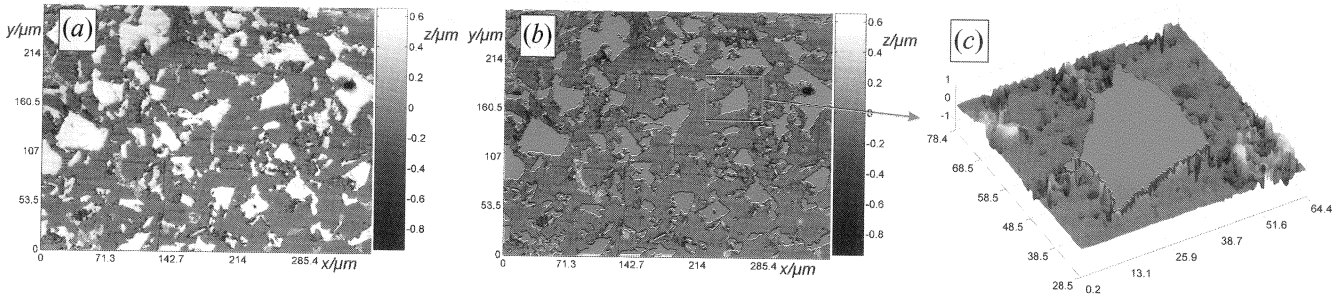

Figure 3. Alusil cylinder liner surface: detection of silicon crystal structures. (*a*) Grey coded height plot; (*b*) peak structures (red) of the surface in (*a*); (*c*) 3D topography plot of one relevant silicon crystal. The border line is located at the steepest connected edge.

The resulting watershed line is located at the steepest connected edge between the structure and the background marker. The watershed line separates the structures from the background and provides the border line of the structure. The watershed transform can provide adjacent structures in one autonomous region which should be connected into a single structure.

The noise sensitivity of the watershed transform and the gradient is reduced by decreasing the space where a resulting watershed line can settle. In this procedure this is achieved by enlarging the markers (figure 2) in contrast to a former version of the detection algorithm [17].

3.1. Detection results

The functionality of the proposed algorithm is shown with a detection of function-relevant structures of very different cylinder liner surfaces. All cylinder liner surface samples shown in this paper are measured with a white light interferometer with an optical set-up with a numerical aperture of 0.4. With all these surfaces, a detection and extraction of characteristic structures are possible. The function-relevant structures are a subset of this detected characteristic structures. The subset is defined by structural parameters [13].

Figure 3(*a*) shows an Alusil [1] cylinder liner surface. Characteristic structures of these surfaces are silicon crystals which are embedded in an aluminium alloy matrix. The silicon crystals are higher than the matrix and provide a wear resistant surface. Detecting the peak structures (figure 3(*b*)) with a subsequent selection of all structures with an areal size $A > 100\,\mu\text{m}^2$ provides the function-relevant structures of this type of surface (figure 3(*c*)).

The detection results of porous surfaces are shown in figure 4. Figure 4(*a*) shows a laser exposed surface [3]. The function-relevant structures of this type of surface are graphite pores which are all detected valley structures with an areal size $A > 300\,\mu\text{m}^2$ and a mean height $h_M > 0.8\,\mu\text{m}$. In figure 4(*c*), a measurement of a laser honed surface [2] is to be seen. The laser hole is function relevant. By detecting all valley structures with a mean height $h_M > 15\,\mu\text{m}$, the laser hole could be selected and evaluated. The function-relevant structures (pores) of a plasma-coated aluminium surface [18] shown in figures 4(*e*) and (*f*) are structures with an areal size $A > 10\,\mu\text{m}^2$ and a mean height $h_M > 0.8\,\mu\text{m}$.

The proposed algorithm turned out to provide quite robust structure detection for rough cylinder liner types of surfaces measured with optical topography instruments as a round robin of optical topography measuring systems showed [19]. A total of 26 profilers (13 white light interferometers, nine confocal microscopes, four miscellaneous) and 11 cylinder liner samples took part in this round robin test. A total of 737 measurements were evaluated with the proposed algorithm and showed very stable detection results. Nonetheless, the definition of stable structure-oriented parameters should avoid using only points of the structure border line.

4. Structure-oriented evaluation of honing angles

Every single detected structure could be described with a set of structural parameters [13]. Statistical combination of a subset of these parameters leads to a functional characterization of the measured surface. The potential of this toolbox can be shown with the example of a honing angle detection.

The surface finishing process honing generates oriented grooves. To describe the quality of the finished surface, the size and the orientation of these honing grooves are relevant.

For the detection of the honing angles, three structural parameters of the surface valley structures are needed:

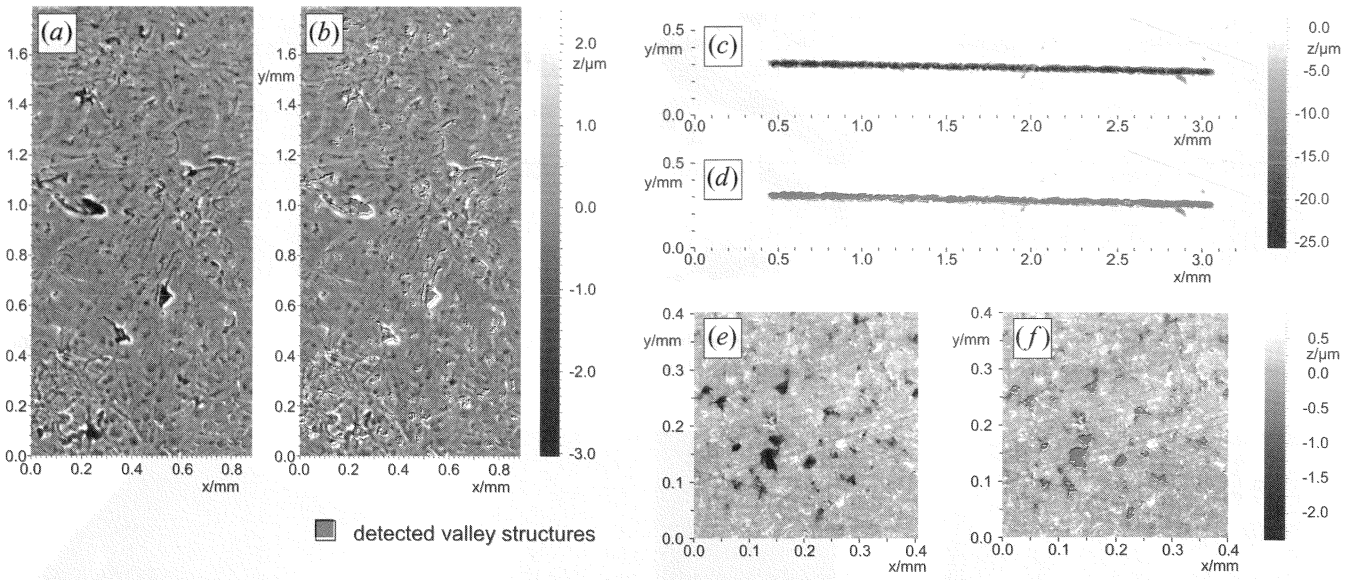

Figure 4. Detection of valley structures: (*a*) grey coded height plot of a laser exposed surface; (*b*) relevant valley structures (pores in red) of the surface in (*a*); (*c*) grey coded height plot of a laser honed surface; (*d*) relevant valley structures (laser holes in red) of surface in (*c*); (*e*) grey coded height plot of a plasma coated surface; (*f*) relevant valley structures (pores in red) of surface in (*e*).

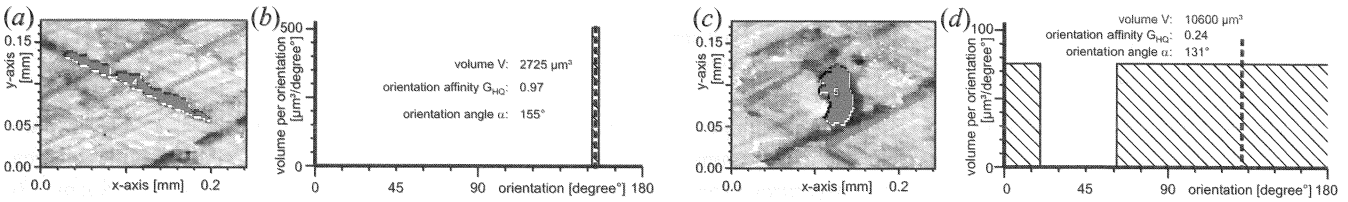

Figure 5. Valley structures of a honed surface with their representation in the histogram: (*a*) distinctive oblong structure; (*b*) rectangular representation of structure in (*a*); (*c*) rather round structure; (*d*) rectangular representation of structure in (*c*).

volume V, orientation angle α and orientation affinity G_{HQ}. The volume of a structure is calculated by summation of the structure point heights h_i multiplied with their lateral dimension Δx and Δy

$$V = \Delta x \Delta y \sum_i h_i. \tag{2}$$

The orientation affinity G_{HQ} of a structure characterizes if it is a distinctive oblong structure (figure 5(*a*): G_{HQ} equal to 0.97) or a rather round structure (figure 5(*c*): G_{HQ} equal to 0.24). Structures with an orientation affinity $G_{\mathrm{HQ}} > 0$ have an orientation direction which can be specified with an orientation angle α. Orientation affinity and orientation angle can be calculated with a fit of straight lines or a Karhunen–Loeve transformation [20].

The eigenvectors of the covariance matrix of the structure points describe the main axes of the structure and the eigenvalues are a measure of the variance in the directions of the main axes. Good calculation results are achieved by additionally weighting the structure points (x, y) with their height $z(x, y)$ to reduce the influence of border line points. The orientation angle is calculated using the eigenvectors and in the special case proposed in this paper the orientation affinity G_{HQ} is calculated using the eigenvalues ev

$$1 - G_{\mathrm{HQ}} = \left[\frac{\min(ev)}{\max(ev)}\right]^{\frac{1}{2}}. \tag{3}$$

A rather simple rectangular model is used to combine the parameters of every structure within a single histogram. This histogram shows on the y-axis volume per orientation and on the x-axis the orientation. The area a rectangle of a structure takes in the histogram is proportional to the volume of the structure (h is the height and b is the width of the rectangle)

$$V = h \cdot b. \tag{4}$$

The width b of the rectangle is defined by the orientation affinity G_{HQ}

$$b = 180°(1 - G_{\mathrm{HQ}}). \tag{5}$$

The orientation angle α defines the centre of the rectangle. The minimum and the maximum angle $b_{\min}$ and $b_{\max}$ are calculated as

$$b_{\max/\min} = \alpha \pm \frac{b}{2}. \tag{6}$$

The angles are wrapped at 0° and 180° by adding or subtracting 180° (angles below zero are increased by adding 180°, angles above 180° are decreased by subtracting 180°). The rectangles for the example structures are shown in figures 5(*b*) and (*d*).

The addition of the rectangles of all structures provide the histogram of the surface (figure 6(*b*)). The size of the region between two given angles is a measure of the amount of oriented volume pointing in that direction. Honed surfaces show local maxima in the histogram which correspond to the honing angles.

With the proposed structure-oriented evaluation, it is possible to identify the structures that are responsible for the

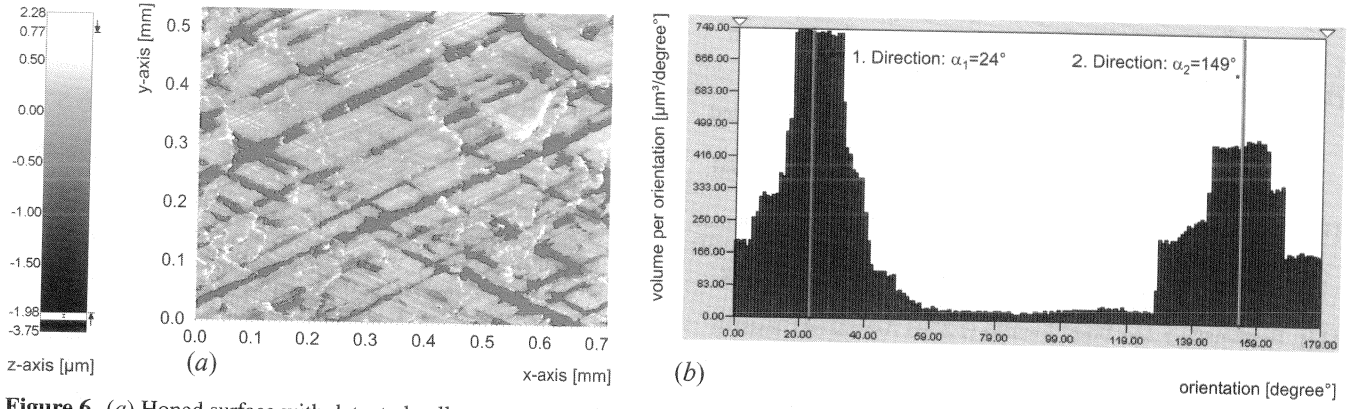

Figure 6. (*a*) Honed surface with detected valley structures; (*b*) histogram of the oriented volumes with significant local maxima corresponding to honing angles.

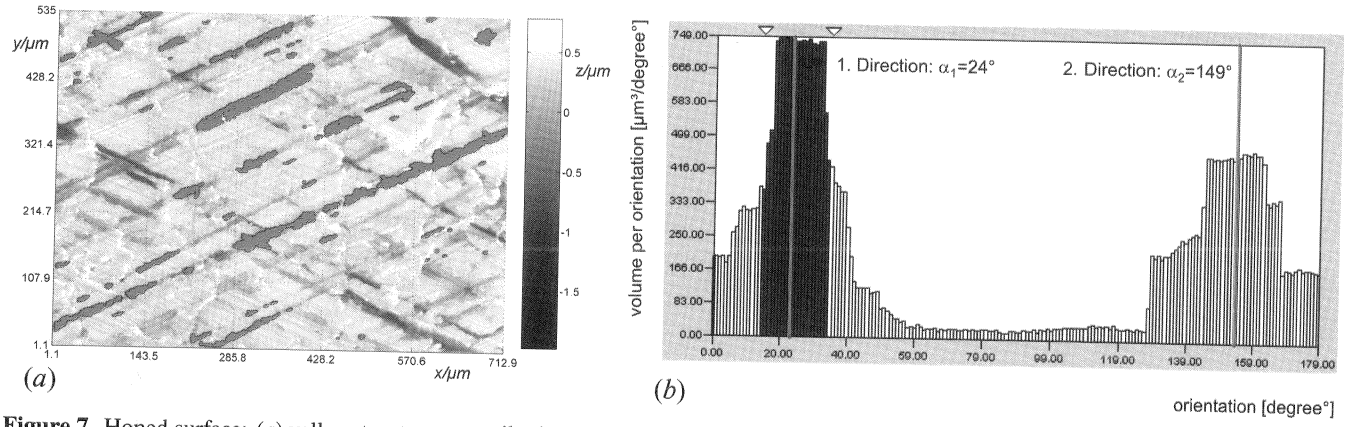

Figure 7. Honed surface: (*a*) valley structures contributing to direction $\alpha = 24°$ are marked; (*b*) histogram of the oriented volumes with the marked direction $\alpha = 24°$.

oriented volume between two given angles. In figure 7, the structures with orientation angles between 17° and 34° are selected. Further processing of the selected structures could evaluate their number, their mean volume and their mean length.

5. Conclusion

Structure-oriented 3D roughness evaluation turned out to be an intuitively usable toolbox to describe technical surfaces. The designer of a surface can combine a subset of the structural parameters to use the additional information of a 3D topography measurement and with that to describe the special functional behaviour of the surface. With tribological critical surfaces like cylinder liners this method provided very good results. Maybe it is possible to extend the use of this method to different types of surfaces.

Acknowledgments

The authors would like to thank the *Arbeitskreis 3D-Rauheitsmesstechnik*: Audi AG: H Lindner; BMW AG: E Kindlein, M Stiebler; DaimlerChrysler AG: Dr N Rau, T Hercke; Dr Ing H C F Porsche AG: B Burger; Federal Mogul GmbH: U Lenhof; Volkswagen AG: Dr J Strobel, Dr U Laudahn, C Neukirch; Institut für Mess- und Regelungstechnik, Uni-Hannover: Professor Dr H Bodschwinna, Dr J Seewig.

References

[1] Köhler E 1994 The KS Lokasil process *Foundry Int.* **17** 3–4
[2] Flores G and Klink U 2002 Gestaltung von tribologischen Flächen durch Laserhonen *13th Int. Colloquium Tribology* vol 3 pp 2365–71
[3] Lindner H, Bergmann W, Reichstein S, Brandenstein C, Lang A, Queitsch R and Stengel E 2002 Präzisionsbearbeitung von Grauguß-Zylinderlaufbahnen von Verbrennungskraftmaschinen mit UV-Photonen *13th Int. Colloquium Tribology on Lubricants, Materials, and Lubrication Engineering* vol 3 pp 2373–96
[4] Stout K J *et al* 1993 *The development of methods for the characterisation of roughness in three dimensions* Office for Official Publications of the European Communities, Luxembourg
[5] Pfestorf M, Engel U and Geiger M 1998 Three-dimensional characterization of surfaces for sheet metal forming *Wear* **216** 244–50
[6] Mandelbrot B B 1983 *The Fractal Geometry of Nature* (San Francisco: Freeman)
[7] Scott P J 2003 Novel area characterisation techniques *Advanced Techniques for Assessment Surface Topography: Development of a Basis for 3D Surface Texture Standards "SURFSTAND"* ed L Blunt and X Jiang (London: Kogan Page Science) pp 43–61
[8] Blunt L, Jiang X, Scott P J and Xiao S 2004 Surface metrology of MST devices *11th. Int. Colloquium on Surfaces, Proc.* vol 1 pp 22–32
[9] Wolf G W 1991 A FORTRAN subroutine for cartographic generalization *Comput. Geosci.* **17** 1359–81
[10] Barre F and Lopez J 2001 On a 3D extension of the MOTIF method (ISO 12085) *Int. J. Mach. Tools Manuf.* **41** 1873–80

[11] Abbott E and Firestone F 1933 Specifying surface quality—a method based on accurate measurement and comparison *Am. Soc. Mech. Eng.* **55** 569–74

[12] ISO13565-2 Geometrical Product Specifications (GPS)—Surface texture: Profile method; Surfaces having stratified functional properties—Part 2: Height characterization using the linear material ratio curve (Geneva, Switzerland 1996)

[13] Weidner A, Seewig J and Lemke H-W 2004 Structure oriented parameters for the function related evaluation of data for 3D surface roughness. *ICS, Int. Colloquium on Surfaces (Int. Oberflächenkolloquium)* vol 11 pp 233–41

[14] Brinkmann S and Bodschwinna H 2003 Advanced Gaussian filters *Advanced Techniques for Assessment Surface Topography: Development of a Basis for 3D Surface Texture Standards "SURFSTAND"* ed L Blunt and X Jiang (London: Kogan Page Science) pp 62–90

[15] Seewig J 2000 Praxisgerechte Signalverarbeitung zur Trennung der Gestaltabweichungen technischer Oberflächen *PhD Thesis* Institute for Measurement and Control, University of Hannover, Hannover, Germany

[16] Soille P 1999 *Morphological Image Analysis: Principles and Applications* (Berlin: Springer)

[17] Lemke H-W, Seewig J, Bodschwinna H and Brinkmann S 2002 Silizium-partikel in Aluminium. Analyse von Zylinderlaufbahnoberflächen *Qualität. Zuverlässigkeit* **47** 1273–7

[18] Hadler J, Flor S and Heikel C 2005 Innovationen aus der Volkswagen Dieselmotorenentwicklung *3. Tagung Gießtechnik im Motorenbau, Anforderungen der Automobilindustrie, VDI-Ges. Werkstofftechnik (Magdeburg, DE, Feb. 2005)* vol 1830 pp 285–308

[19] Weidner A, Seewig J and Reithmeier E 2005 Structure oriented 3D roughness evaluation with optical profilers *Proc. 10th Int. Conf. on Metrology and Properties of Engineering Surfaces (St Etienne, France, July 2005) (ENISE)* ed T Thomas, B G Rosen and H Zahouani pp 49–58

[20] Loeve M 1963 *Probability Theory* 3rd edn (Princeton, NJ: van Nostrand)